

Cluster representations and the Wolff algorithm in arbitrary external fields

Jaron Kent-Dobias and James P. Sethna

Laboratory of Atomic and Solid State Physics, Cornell University, Ithaca, New York 14853-2501, USA

(Received 16 May 2018; published 7 December 2018)

We introduce a natural way to extend celebrated spin-cluster Monte Carlo algorithms for fast thermal lattice simulations at criticality, such as the Wolff algorithm, to systems in arbitrary fields, be they linear magnetic vector fields or nonlinear anisotropic ones. By generalizing the “ghost spin” representation to one with a “ghost transformation,” global invariance to spin symmetry transformations is restored at the cost of an extra degree of freedom which lives in the space of symmetry transformations. The ordinary cluster-building process can then be run on the representation. We show that this extension preserves the scaling of accelerated dynamics in the absence of a field for Ising, Potts, and $O(n)$ models and demonstrate the method’s use in modeling the presence of novel nonlinear fields. We also provide a C++ library for the method’s convenient implementation for arbitrary models.

DOI: [10.1103/PhysRevE.98.063306](https://doi.org/10.1103/PhysRevE.98.063306)**I. INTRODUCTION**

Lattice models are important in the study of statistical physics and phase transitions. Rarely exactly solvable, they are typically studied by approximate and numerical methods. Monte Carlo techniques are a common way of doing this, approximating thermodynamic quantities by sampling the distribution of system states. These Monte Carlo algorithms are better the faster they arrive at a statistically independent sample. This becomes a problem near critical points where critical slowing down [1] results in power-law divergences of dynamic timescales.

Celebrated cluster algorithms largely addressed this in the absence of symmetry-breaking fields by using nonlocal updates [2] whose clusters undergo a percolation transition at the critical point of the system [3]. These result in relatively small dynamic exponents for many spin systems [4–7], including the Ising, $O(n)$ [8], and Potts [9,10] models. These algorithms rely on the natural invariance of the systems in question under symmetry transformations on their spins.

Some success has been made in extending these algorithms to systems in certain external fields by adding a “ghost site” [11] that returns global rotation invariance to spin Hamiltonians at the cost of an extra degree of freedom, allowing the method to be used in a subcategory of interesting fields [12–14]. Static fields have also been applied by including a separate metropolis or heat bath update step after cluster formation [15–17], and other categories of fields have been applied using replica methods [18–20]. Monte Carlo techniques that involve cluster updates at fixed magnetization have been used to examine quantities at fixed field by later integrating measured thermodynamic functions [21,22].

We show that the scaling of correlation time near the critical point of several models suggests that the ghost approach is a natural one, e.g., that it extends the celebrated scaling of dynamics in these algorithms at zero fields to various nonsymmetric perturbations. We also show, by a redefinition

of the spin-spin coupling in a generic class of spin systems, *arbitrary* external fields can be treated using cluster methods. Rather than the introduction of a ghost spin, our representation relies on introducing a “ghost transformation,” an extra degree of freedom residing on a ghost site coupled to all other sites that takes its values from the collection of spin symmetry transformations of the base model rather than resemble the base spins themselves.

We provide an open-source implementation of this method in the form of a C++ library, available in Ref. [23]. Use of this library will be described briefly within, but extensive documentation is also available Ref. [23].

II. CLUSTERS WITHOUT A FIELD

We will pose the problem in a general way, but several specific examples can be found in Table I for concreteness. Let $G = (V, E)$ be a graph where the set of vertices $V = \{1, \dots, N\}$ enumerates the sites of a lattice and the set of edges E contains pairs of neighboring sites. Let R be a group acting on a set X with the action of group elements $r \in R$ on elements $s \in X$ denoted $r \star s$. X is the set of states accessible by each spin, and R is the *symmetry group* of X . The set X must admit a measure μ that is invariant under the action of R , e.g., for any $A \subseteq X$ and $r \in R$, $\mu(r \star A) = \mu(A)$. This trait is shared by the counting measure on any discrete set or by any group acting by isometries on a Riemannian manifold, such as $O(n)$ on S^{n-1} in the $O(n)$ models [24]. Finally, a subset R_2 of elements in R of order two must act transitively on X . This property, although apparently obscure, is shared by any symmetric space [25] or by any transitive finitely generated isometry group. In fact, all the examples listed here have spin spaces with natural metrics whose symmetry group is their set of isometries. We put one spin at each site of the lattice described by G so that the state of the entire system is described by elements $\mathbf{s} \in X \times \dots \times X = X^N$.

TABLE I. Several examples of spin systems and the symmetry groups that act on them. Common choices for the spin-spin coupling in these systems and their external fields are also given. Other fields are possible, of course: For instance, some are interested in modulated fields $H \cos[2\pi k\theta(s)]$ for integer k and $\theta(s)$ giving the angle of s to some axis applied to the $O(2)$ model [27]. All models listed here have example implementations in the provided C++ library [23].

	Spins (X)	Symmetry (R)	Action ($g \star s$)	Coupling [$Z(s, t)$]	Common field [$B(s)$]
Ising	$\{-1, 1\}$	$\mathbb{Z}/2\mathbb{Z}$	$0 \star s \mapsto s, 1 \star s \mapsto -s$	st	Hs
$O(n)$	S^{n-1}	$O(n)$	$M \star s \mapsto Ms$	$s \cdot t$	$H \cdot s$
Potts	$\{1, \dots, q\}$	S_n	$(i_1, \dots, i_q) \star s = i_s$	$\delta(s, t)$	$\sum_m H_m \delta(m, s)$
Clock	$\mathbb{Z}/q\mathbb{Z}$	D_n	$r_m \star s = m + s, s_m \star s = -m - s$	$\cos(2\pi \frac{s-t}{q})$	$\sum_m H_m \cos(2\pi \frac{s-m}{q})$
DGM	\mathbb{Z}	D_{inf}	$r_m \star s = m + s, s_m \star s = -m - s$	$(s - t)^2$	Hs^2

The Hamiltonian of this system is a function $\mathcal{H}: X^N \rightarrow \mathbb{R}$ defined by

$$\mathcal{H}(\mathbf{s}) = - \sum_{\{i, j\} \in E} Z(s_i, s_j) - \sum_{i \in V} B(s_i), \tag{1}$$

where $Z: X \times X \rightarrow \mathbb{R}$ couples adjacent spins and $B: X \rightarrow \mathbb{R}$ is an external field. Z must be symmetric in its arguments and invariant under the action of any element of R applied to the entire lattice, that is, for any $r \in R$ and $s, t \in X$, $Z(r \star s, r \star t) = Z(s, t)$. One may also allow Z to be a function of edge—for modeling random-bond, long-range, or anisotropic interactions—or allow B to be a function of site—for applying arbitrary boundary conditions or modeling random fields. The formal results of this paper (that the algorithm obeys detailed balance and ergodicity) hold equally well for these cases, but we will drop the additional index notation for clarity. Some extensions, such as adding strong random fields or bonds, ultimately prove inefficient [18,26].

Implementation of a model in the provided library is as simple as defining a class that represents an element of the state space X with a default constructor (and destructor, if necessary) and a class that represents an element of the group R with a default constructor and member functions that define the action and inverse action of the class in both states and group elements. Specific details may be found in Ref. [23].

The goal of statistical mechanics is to compute expectation values of observables $A: X^N \rightarrow \mathbb{R}$. Assuming the ergodic hypothesis holds (for systems with broken-symmetry states, it does not), the expected value $\langle A \rangle$ of an observable A is its average over every state \mathbf{s} in the configuration space X^N weighted by the Boltzmann probability of that state appearing, or

$$\langle A \rangle = \frac{\int_{X^N} A(\mathbf{s}) e^{-\beta \mathcal{H}(\mathbf{s})} d\mu(\mathbf{s})}{\int_{X^N} e^{-\beta \mathcal{H}(\mathbf{s})} d\mu(\mathbf{s})}, \tag{2}$$

where for $Y_1 \times \dots \times Y_N = Y \subseteq X^N$ the product measure $\mu(Y) = \mu(Y_1) \dots \mu(Y_N)$ is the simple extension of the measure on X to a measure on X^N . These values are estimated using Monte Carlo techniques by constructing a finite sequence of states $\{\mathbf{s}_1, \dots, \mathbf{s}_M\}$ such that

$$\langle A \rangle \simeq \frac{1}{M} \sum_{i=1}^M A(\mathbf{s}_i). \tag{3}$$

Sufficient conditions for this average to converge to $\langle A \rangle$ as $M \rightarrow \infty$ are that the process that selects \mathbf{s}_{i+1} given the previous states be Markovian (only depends on \mathbf{s}_i), ergodic (any state can be accessed), and obey detailed balance (the ratio of probabilities that \mathbf{s}' follows \mathbf{s} and vice versa is equal to the ratio of weights for \mathbf{s} and \mathbf{s}' in the ensemble).

Measurements of observables during Monte Carlo techniques in the provided library are made by the use of hooks, which are member functions of a measurement class that are run at designated points during the algorithm’s execution and provide arbitrary information about the internal state of all relevant objects. A detailed description of these hooks can be found in Ref. [23].

Although any of several related cluster algorithms can be described for this system, we will focus on the Wolff algorithm [8]. In the absence of an external field, e.g., $B(s) = 0$, the Wolff algorithm proceeds in the following way.

Algorithm 1. Wolf

1. Pick a random site m_0 , and add it to the stack.
 2. Select a transformation $r \in R_2$ distributed by $f(r|m_0, \mathbf{s})$. Often, f is taken as uniform on R_2 , but it is sufficient for preserving a detailed balance that f be any function of the seed site m_0 and $Z(s, r \star s)$ for all $s \in \mathbf{s}$. The flexibility offered by the choice of distribution will be useful in situations where the set of spin states is infinite.
 3. While the stack is not empty,
 - (a) pop site m from the stack.
 - (b) If site m is not marked,
 - i. mark the site.
 - ii. For every j such that $\{m, j\} \in E$, add site j to the stack with probability,

$$p_r(s_m, s_j) = \min\{0, 1 - e^{\beta[Z(r \star s_m, s_j) - Z(s_m, s_j)]}\}. \tag{4}$$
 - iii. Take $s_m \mapsto r \star s_m$.
-

When the stack is exhausted, a cluster of connected spins will have been transformed by the action of r . In order for this algorithm to be useful, it must satisfy ergodicity and detailed balance. Ergodicity is satisfied since we have ensured that R_2 acts transitively on X , e.g., for any $s, t \in X$, there exists $r \in R_2$ such that $r \star s = t$. Since there is a nonzero probability that only one spin is transformed and that spin can be transformed into any state, ergodicity follows. The probability $P(\mathbf{s} \rightarrow \mathbf{s}')$ that configuration \mathbf{s} is brought to \mathbf{s}' by the flipping of a cluster

formed by accepting transformations of spins via bonds $C \subseteq E$ and rejecting transformations via bonds $\partial C \subset E$ is related to the probability of the reverse process $P(\mathbf{s}' \rightarrow \mathbf{s})$ by

$$\begin{aligned} \frac{P(\mathbf{s} \rightarrow \mathbf{s}')}{P(\mathbf{s}' \rightarrow \mathbf{s})} &= \frac{f(r|m_0, \mathbf{s})}{f(r^{-1}|m_0, \mathbf{s}')} \prod_{\{i,j\} \in C} \frac{p_r(s_i, s_j)}{p_{r^{-1}}(s'_i, s'_j)} \\ &\times \prod_{\{i,j\} \in \partial C} \frac{1 - p_r(s_i, s_j)}{1 - p_{r^{-1}}(s'_i, s'_j)} \\ &= \prod_{\{i,j\} \in \partial C} e^{\beta[Z(s'_i, s'_j) - Z(s_i, s_j)]} \\ &= \frac{e^{-\beta \mathcal{H}(\mathbf{s}')}}{e^{-\beta \mathcal{H}(\mathbf{s})}}, \end{aligned} \tag{5}$$

whence detailed balance is also satisfied, using $r = r^{-1}$ and $Z(r \star s', s') = Z(r \star s, s)$.

The Wolff algorithm is well known to be efficient in sampling many spin models near and away from criticality, including the Ising, Potts, and $O(n)$ models. In general, its efficiency will depend on the system at hand, e.g., the structure of the configurations X and group R . A detailed discussion of this dependence for a class of configuration spaces with continuous symmetry groups can be found in Refs. [24,28].

This algorithm can be run on a system using the provided library. To construct a system, you must provide a graph representing the lattice, the temperature, the spin coupling function Z , and the field coupling function B . Once constructed, cluster flips as described in the algorithm can be performed by directly providing seed sites m_0 and transformations r or many in sequence by providing a function that generates random (appropriately distributed to preserve detailed balance) transformations r . The construction and use of Wolff systems is described Ref. [23].

III. ADDING THE FIELD

This algorithm relies on the fact that the coupling Z depends only on relative orientation of the spins—global reorientations do not affect the Hamiltonian. The external field B breaks this symmetry. Fortunately, it can be restored. Define a new graph $\tilde{G} = (\tilde{V}, \tilde{E})$, where $\tilde{V} = \{0, 1, \dots, N\}$ adds the new ghost site 0 which is connected by

$$\tilde{E} = E \cup \{\{0, i\} | i \in V\} \tag{6}$$

to all other sites. Instead of assigning the ghost site a spin whose value comes from X , we assign it values in the symmetry group $s_0 \in R$ so that the configuration space of the new model is $R \times X^N$. We introduce the Hamiltonian $\tilde{\mathcal{H}}: R \times X^N \rightarrow \mathbb{R}$ defined by

$$\begin{aligned} \tilde{\mathcal{H}}(s_0, \mathbf{s}) &= - \sum_{\{i,j\} \in E} Z(s_i, s_j) - \sum_{i \in V} B(s_0^{-1} \star s_i) \\ &= - \sum_{\{i,j\} \in \tilde{E}} \tilde{Z}(s_i, s_j), \end{aligned} \tag{7}$$

where the new coupling $\tilde{Z}: (R \cup X) \times (R \cup X) \rightarrow \mathbb{R}$ is defined for $s, t \in R \cup X$ by

$$\tilde{Z}(s, t) = \begin{cases} Z(s, t), & \text{if } s, t \in X, \\ B(s^{-1} \star t), & \text{if } s \in R, \\ B(t^{-1} \star s), & \text{if } t \in R. \end{cases} \tag{8}$$

The modified coupling is invariant under the action of group elements: For any $r, s_0 \in R$ and $s \in X$,

$$\begin{aligned} \tilde{Z}(rs_0, r \star s) &= B[(rs_0)^{-1} \star (r \star s)] \\ &= B(s_0^{-1} \star s) \\ &= \tilde{Z}(s_0, s). \end{aligned} \tag{9}$$

The invariance of \tilde{Z} to global transformations given other arguments follows from the invariance properties of Z .

We have produced a system incorporating the field function B whose Hamiltonian is invariant under global rotations, but how does it relate to our old system, whose properties we actually want to measure? If $A: X^N \rightarrow \mathbb{R}$ is an observable of the original system, we construct an observable $\tilde{A}: R \times X^N \rightarrow \mathbb{R}$ of the new system defined by

$$\tilde{A}(s_0, \mathbf{s}) = A(s_0^{-1} \star \mathbf{s}), \tag{10}$$

whose expectation value in the new system equals that of the original observable in the old system. First, note that $\tilde{\mathcal{H}}(1, \mathbf{s}) = \mathcal{H}(\mathbf{s})$. Since the Hamiltonian is invariant under global rotations, it follows that, for any $g \in R$, $\tilde{\mathcal{H}}(g, g \star \mathbf{s}) = \mathcal{H}(\mathbf{s})$. Using the invariance properties of the measure on X and introducing a measure ρ on R , it follows that:

$$\begin{aligned} \langle \tilde{A} \rangle &= \frac{\int_R \int_{X^N} \tilde{A}(s_0, \mathbf{s}) e^{-\beta \tilde{\mathcal{H}}(s_0, \mathbf{s})} d\mu(\mathbf{s}) d\rho(s_0)}{\int_R \int_{X^N} e^{-\beta \tilde{\mathcal{H}}(s_0, \mathbf{s})} d\mu(\mathbf{s}) d\rho(s_0)} \\ &= \frac{\int_R \int_{X^N} A(s_0^{-1} \star \mathbf{s}) e^{-\beta \tilde{\mathcal{H}}(s_0, \mathbf{s})} d\mu(\mathbf{s}) d\rho(s_0)}{\int_R \int_{X^N} e^{-\beta \tilde{\mathcal{H}}(s_0, \mathbf{s})} d\mu(\mathbf{s}) d\rho(s_0)} \\ &= \frac{\int_R \int_{X^N} A(\mathbf{s}') e^{-\beta \tilde{\mathcal{H}}(s_0, s_0 \star \mathbf{s}')} d\mu(s_0 \star \mathbf{s}') d\rho(s_0)}{\int_R \int_{X^N} e^{-\beta \tilde{\mathcal{H}}(s_0, s_0 \star \mathbf{s}')} d\mu(s_0 \star \mathbf{s}') d\rho(s_0)} \\ &= \frac{\int_R d\rho(s_0) \int_{X^N} A(\mathbf{s}') e^{-\beta \mathcal{H}(\mathbf{s}')} d\mu(\mathbf{s}')}{\int_R d\rho(s_0) \int_{X^N} e^{-\beta \mathcal{H}(\mathbf{s}')} d\mu(\mathbf{s}')} \\ &= \langle A \rangle. \end{aligned} \tag{11}$$

Using this equivalence, spin systems in a field may be treated in the following way.

- (1) Add a site to your lattice adjacent to every other site.
- (2) Initialize a spin at that site whose value is a representation of a member of the symmetry group of your ordinary spins.
- (3) Carry out the ordinary Wolff cluster-flip procedure on this new lattice, substituting \tilde{Z} as defined in (8) for Z .

Ensemble averages of observables A can then be estimated by sampling the value of \tilde{A} on the new system. In contrast with the simpler ghost spin representation, this form of the Hamiltonian might be considered the ghost transformation representation.

One of the celebrated features of the cluster representation of the Ising and associated models is the improved estimators of various quantities in the base model, found by measuring conjugate properties of the clusters themselves [29]. How many of these quantities survive this translation? As is noted in the formative construction of the cluster representation for the Ising and Potts models, all estimators involving correlators between spins are preserved, including correlators with the ghost site [30]. Where a previous improved estimator exists, we expect this representation to extend it to finite fields, all other features of the algorithm hold constant. For instance, the average cluster size in the Wolff algorithm is often said to be an estimator for the magnetic susceptibility in the Ising, Potts, and (with clusters weighted by the components of their spins along the reflection direction [31]) $O(n)$ models, but really what it estimates is the averaged squared magnetization, which corresponds to the susceptibility when the average magnetization is zero. At finite fields, the latter is no longer true, but the correspondence between the cluster size and the squared magnetization continues to hold [see (16) and Fig. 3 below].

IV. EXAMPLES

Several specific examples from Table I are described in the following.

A. The Ising model

In the Ising model, spins are drawn from set $\{1, -1\}$. Its symmetry group is C_2 , the cyclic group on two elements, which can be conveniently represented by a multiplicative group with elements $\{1, -1\}$, exactly the same as the spins themselves. The only nontrivial element is of order two and is selected every time in the algorithm. Since the symmetry group and the spins are described by the same elements, performing the algorithm on the Ising model in a field is fully described by just using the ghost spin representation. This algorithm or algorithms based on the same decomposition of the Hamiltonian have been applied by several researchers [12–14]. The algorithm has been implemented by one of the authors in an existing interactive Ising simulator in Ref. [32].

B. The $O(n)$ models

In the $O(n)$ model, spins are described by vectors on the $(n - 1)$ -sphere S^{n-1} . Its symmetry group is $O(n)$, $n \times n$ orthogonal matrices, which act on the spins by matrix multiplication. The elements of $O(n)$ of order two are reflections about hyperplanes through the origin and π rotations about any axis through the origin. Since the former generate the entire group, reflections alone suffice to provide ergodicity. Sampling those reflections uniformly works well at criticality. The ghost spin version of the algorithm has been used to apply a simple vector field to the $O(3)$ model [33]. Other fields of interest include $(n + 1)$ -dimensional spherical harmonics [27] and cubic fields [34,35], which can be applied with the new method. The method is quickly generalized to spins whose symmetry groups are other compact Lie groups [24,28].

At low temperatures or high external vector fields, selecting reflections uniformly becomes inefficient because the

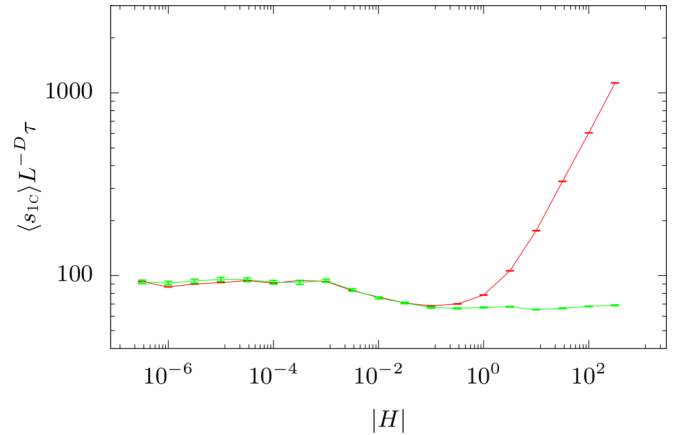


FIG. 1. The scaled autocorrelation time of the energy \mathcal{H} for the Wolff algorithm on a $32 \times 32 \times 32$ XY model at its critical temperature as a function of applied vector field magnitude $|H|$. The red points correspond to reflections sampled uniformly, whereas the green points represent reflections sampled as described in Sec. IV B.

excitations of the model are spin waves in which the magnetization only differs by a small amount between neighboring spins. Under these conditions, most choices of the reflection plane will cause a change in energy so great that the whole system is always flipped, resulting in many correlated samples. To ameliorate this, one can draw reflections from a distribution that depends on how the seed spin is transformed, taking advantage of the freedom to choose the function f in the algorithm. We implement this in the following way. Say that the state of the seed of the cluster is s . Generate a vector t taken uniformly from the space of unit vectors orthogonal to s . Let the plane of reflection be that whose normal is $n = s + \zeta t$, where ζ is drawn from a normal distribution of mean zero and variance σ . It follows that the tangent of the angle between s and the plane of reflection is also distributed normally with zero mean and variance σ . Since the distribution of reflection planes only depends on the angle between s and the plane and since that angle is invariant under the reflection, this choice preserves detailed balance.

The choice of σ can be inspired by mean field theory. At high fields or low temperatures, spins are likely to both align with the field and each other, and the model is asymptotically equal to a simple Gaussian one in which in the limit of large L the expected square angle between neighbors is

$$\langle \theta^2 \rangle \simeq \frac{(n - 1)T}{D + H/2}. \tag{12}$$

We take $\sigma = \sqrt{\langle \theta^2 \rangle} / 2$. Figure 1 shows the effect of making such a choice on autocorrelation times for the energy for a critical three-dimensional (3D) XY [$O(2)$] model. At small fields both methods perform the same as the zero field Wolff algorithm. Intermediate field values see efficiency gains for both methods. At large fields the uniform sampling method sees correlation times grow rapidly without bound, whereas for the sampling method described here the correlation time crosses over to a constant. A similar behavior holds for the critical $O(3)$ model, although in that case the constant value the correlation time approaches at large fields is larger than its

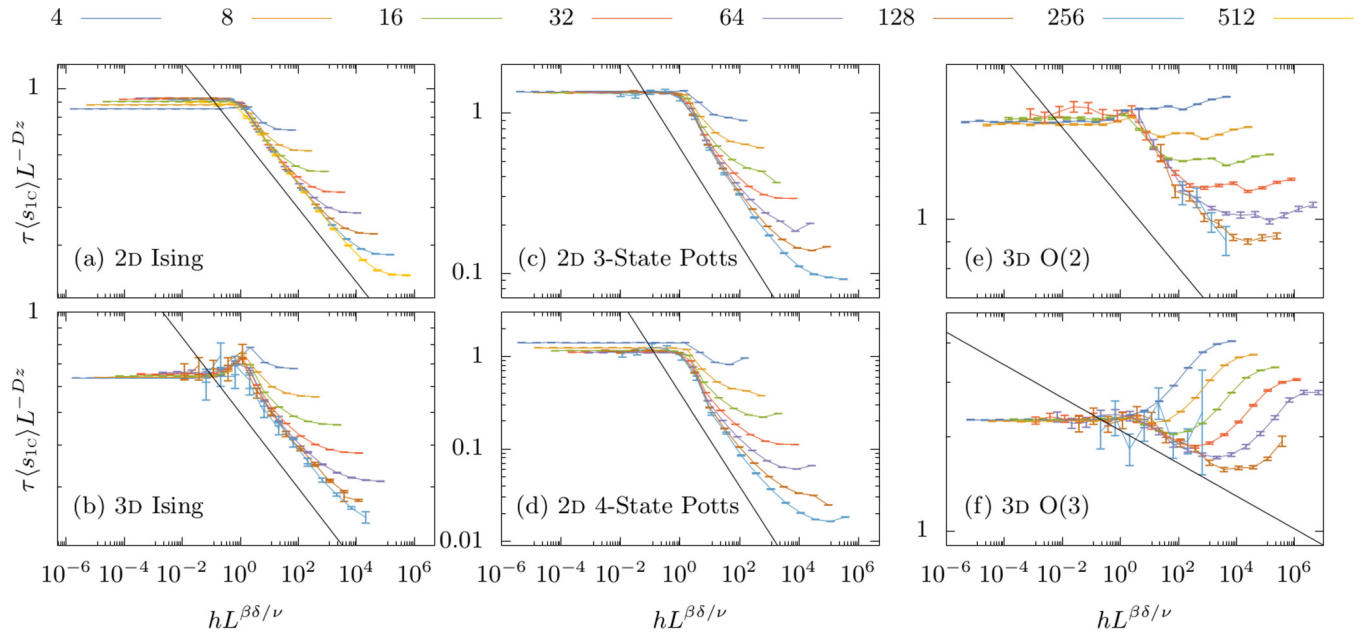


FIG. 2. Scaling collapse of autocorrelation times τ for the energy \mathcal{H} scaled by the average cluster size as a function of an external field for various models of Table I. Critical exponents are model dependent. The colored lines and points depict values as measured by the extended algorithm. The solid black lines show a plot proportional to $h^{-z\nu/\beta\delta}$ for each model. The dynamic exponents z are roughly measured as two-dimensional (2D) Ising: 0.23(5); 3D Ising: 0.28(5); 2D three-state Potts: 0.55(5); 2D four-state Potts: 0.94(5); 3D O(2): 0.17(5); 3D O(3): 0.13(5). $O(n)$ models use the distribution of transformations described in Sec. IV B. The curves stop collapsing at high fields when the correlation length falls near the lattice spacing; here noncluster algorithms can be efficiently used.

minimum value (see Fig. 2). This behavior is not particularly worrisome since the very large field regime corresponds to correlation lengths comparable to the lattice spacing and is efficiently simulated by other algorithms. A more detailed discussion on correlation times and these numeric experiments can be found in Sec. V.

C. The Potts model

In the q -state Potts model, spins are described by elements of $\{1, \dots, q\}$. Its symmetry group is the symmetric group S_n of permutations of its elements. The element (i_1, \dots, i_q) takes the spin s to i_s . There are potentially many elements of order two, but the two-element swaps alone are sufficient to both generate the group and act transitively on $\{1, \dots, q\}$, providing ergodicity.

D. Clock models

In the q -state clock model, spins are described by elements of $\mathbb{Z}/q\mathbb{Z}$, the set of integers mod q . Its symmetry group is the dihedral group $D_q = \{r_0, \dots, r_{q-1}, s_0, \dots, s_{q-1}\}$, the group of symmetries of a regular q -gon. The element r_n represents a rotation by $2\pi n/q$, and the element s_n represents a reflection composed with the rotation r_n . The group acts on spins by permutation: $r_n \star m = n + m \pmod{q}$ and $s_n \star m = -(n + m) \pmod{q}$. This is the natural action of the group on the vertices of a regular polygon that have been numbered 0 through $q - 1$. The elements of D_q of order 2 are all reflections, and $r_{q/2}$ if q is even, although the former can generate the latter. Although reflections do not necessarily

generate the entire group, their action on $\mathbb{Z}/q\mathbb{Z}$ is transitive, and therefore the algorithm is ergodic.

E. Roughening models

Although not often thought of as a spin model, roughening of surfaces can be described in this framework. Spins are described by integers \mathbb{Z} , and their symmetry group is the infinite dihedral group $D_\infty = \{r_i, s_i | i \in \mathbb{Z}\}$, whose action on the spin $j \in \mathbb{Z}$ is given by $r_i \star j = i + j$ and $s_i \star j = -i - j$. The elements of order two are reflections s_i , whose action on \mathbb{Z} is transitive. The coupling can be any function of the absolute difference $|i - j|$. Because the uniform choice of reflection will almost always result in energy changes so large that the whole system is flipped, it is better to select random reflections about integers or half-integers close to the state of the system. A variant of the algorithm has been applied without a field whose success relies both on this and on another technique [36]. They note that detailed balance is still satisfied if the bond probabilities (4) are modified by adding a constant $0 < x \leq 1$ with

$$p_r(s_m, s_j | x) = \min \{0, 1 - x e^{\beta[Z(r \star s_m, s_j) - Z(s_m, s_j)]}\}. \quad (13)$$

When $x < 1$ transformations that do not change the energy of a bond can still activate it in the cluster, they allow nontrivial clusters to be seeded when the height of the starting site is also the plane of reflection. This modification is likely useful, in general, for systems with large yet discrete state spaces.

V. PERFORMANCE

No algorithm is worthwhile if it does not run efficiently. This algorithm, being an extension of the Wolff algorithm into a new domain, should be considered successful if it likewise extends the efficiency of the Wolff algorithm into that domain. Some systems are not efficient under the Wolff algorithm, and we do not expect them to fare better when extended in a field. For instance, Ising models with random fields or bonds technically can be treated with the Wolff algorithm [37], but it is not efficient because the clusters formed do not scale naturally with the correlation length [18,26]. Other approaches, such as replica methods, should be relied on instead [18–20].

At a critical point, correlation time τ scales with system size $L = N^D$ as $\tau \sim L^z$. Cluster algorithms are celebrated for their small dynamic exponents z . In the vicinity of an ordinary critical point, the renormalization group predicts scaling behavior for the correlation time as a function of temperature t and field h of the form

$$\tau = h^{-z\nu/\beta\delta} \mathcal{T}(ht^{-\beta\delta}, hL^{\beta\delta/\nu}). \quad (14)$$

If a given dynamics for a system at a zero field results in scaling, such as L^z , one should expect its natural extension in the presence of a field to scale roughly, such as $h^{-z\nu/\beta\delta}$, and collapse appropriately as a function of $hL^{\beta\delta/\nu}$.

We measured the autocorrelation time τ of the energy \mathcal{H} for a variety of models at critical temperatures with many system sizes and canonical fields (see Table I with $h = \beta H$) using standard methods for obtaining the value and uncertainty from the time series [38]. Since the computational effort expended in each step of the algorithm depends linearly on the size of the associated cluster, these values are then scaled by the average cluster size per site $\langle s_{1c} \rangle / L^D$ to produce

something proportional to machine time per site. The resulting scaling behavior, plotted in Fig. 2, is indeed consistent with an extension to finite fields of the behavior at zero fields with an eventual finite-size crossover to constant autocorrelation time at large fields. This crossover is not always kind to the efficiency, e.g., in the O(3) model, but in the large-field regime where the crossover happens, the correlation length is on the scale of the lattice spacing and better algorithms exist, such as the Bortz-Kalos-Lebowitz algorithm for the Ising model [39]. Also plotted are lines proportional to $h^{-z\nu/\beta\delta}$, which match the behavior of the correlation times in the intermediate scaling region as expected. Values of the critical exponents for the models were taken from the literature [40–42] with the exception of z for the energy in the Wolff algorithm, which was determined for each model by making a power-law fit to the constant low-field behavior. These exponents are imprecise and are provided in the figure with only qualitative uncertainty.

Since the formation and flipping of clusters is the hallmark of Wolff dynamics, another way to ensure that the dynamics with field scales like those without is to analyze the distribution of cluster sizes. The success of the algorithm at zero fields is related to the fact that the clusters formed undergo a percolation transition at the models' critical points. According to the scaling theory of percolation [43], the distribution of cluster sizes in a full Swendsen-Wang decomposition—where the whole system is decomposed into clusters with every bond activated with probability (4)—of the system scales consistently near the critical point if it has the form

$$P_{\text{Sw}}(s) = s^{-\tau} f(ts^\sigma, th^{-1/\beta\delta}, tL^{1/\nu}). \quad (15)$$

The distribution of cluster sizes in the Wolff algorithm can be computed from this using the fact that the algorithm selects

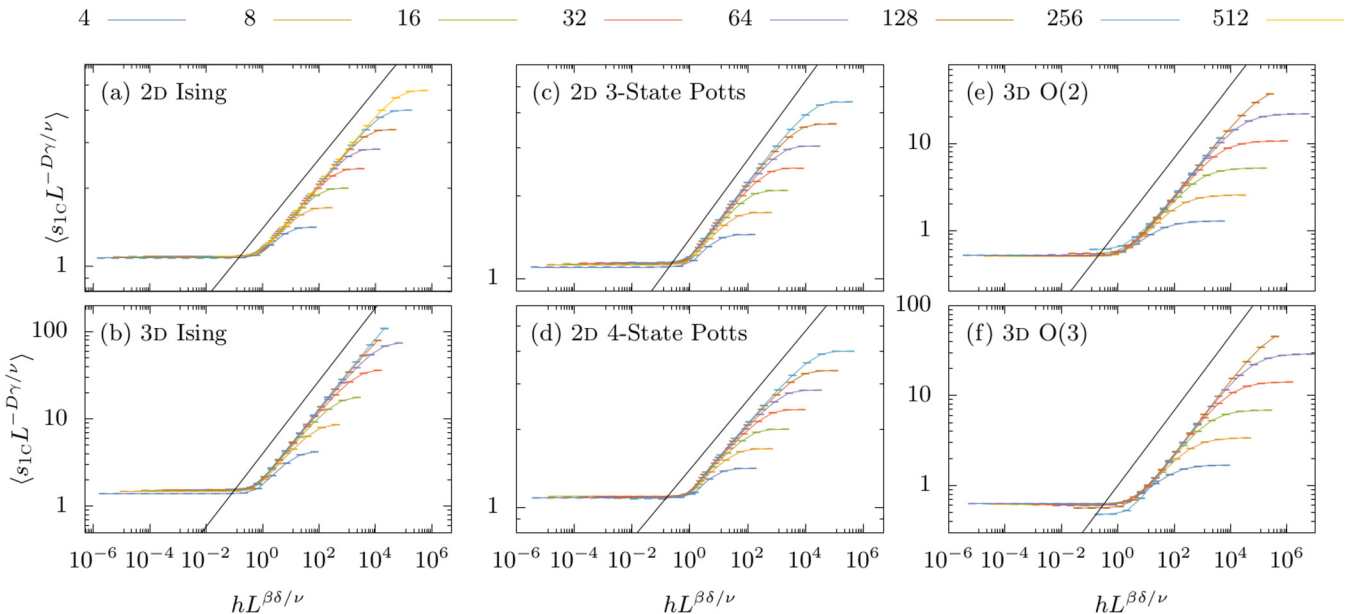


FIG. 3. Collapses of rescaled average Wolff cluster size $\langle s \rangle_{1c} L^{-\gamma/\nu}$ as a function of field scaling variable $hL^{\beta\delta/\nu}$ for a variety of models. Critical exponents γ , ν , β , and δ are model dependant. The colored lines and points depict values as measured by the extended algorithm. The solid black lines show a plot of $g(0, x) \propto x^{2/\delta}$ for each model.

clusters with probability proportional to their size, or

$$\begin{aligned}
 \langle s_{1c} \rangle &= \sum_s s P_{1c}(s) \\
 &= \sum_s s \frac{s}{N} P_{sw}(s) \\
 &= L^{\gamma/\nu} g(ht^{-\beta\delta}, hL^{\beta\delta/\nu}). \quad (16)
 \end{aligned}$$

For the Ising model, an additional scaling relation can be written. Since the average cluster size is the average squared magnetization, it can be related to the scaling functions of the magnetization and susceptibility per site by (with $ht^{-\beta\delta}$ dependence dropped)

$$\begin{aligned}
 \langle s_{1c} \rangle &= L^D \langle M^2 \rangle = \beta \langle \chi \rangle + L^D \langle M \rangle^2 \\
 &= L^{\gamma/\nu} [(hL^{\beta\delta/\nu})^{-\gamma/\beta\delta} \beta \mathcal{Y}(hL^{\beta\delta/\nu}, ht^{-\beta\delta}) \\
 &\quad + (hL^{\beta\delta/\nu})^{2/\delta} \mathcal{M}(hL^{\beta\delta/\nu}, ht^{-\beta\delta})]. \quad (17)
 \end{aligned}$$

We therefore expect that, for the Ising model, $\langle s_{1c} \rangle L^{-\gamma/\nu}$ should go as $(hL^{\beta\delta/\nu})^{2/\delta}$ for large arguments. We further conjecture that this scaling behavior should hold for other models whose critical points correspond with the percolation transition of Wolff clusters. This behavior is supported by our numeric work along the critical isotherm for the various Ising, Potts, and $O(n)$ models, shown in Fig. 3. Fields are the canonical ones referenced in Table I. As can be seen, the average cluster size collapses for each model according to the scaling hypothesis, and the large-field behavior likewise scales as we expect from the naive Ising conjecture.

VI. APPLYING NONLINEAR FIELDS TO THE XY MODEL

Thus far our numeric work has quantified the performance of existing techniques. Briefly, we demonstrate our general framework in a different way: harmonic perturbations to the low-temperature XY, or 2D $O(2)$, model. We consider fields of the form $B_n(s) = h_n \cos[n\theta(s)]$, where θ is the angle made between s and the x axis. Corrections of these types are expected to appear in realistic models of systems naively expected to exhibit Kosterlitz-Thouless critical behavior due to the presence of the lattice or substrate. Whether these fields are relevant or irrelevant in the renormalization group sense determines whether those systems spoil or admit that critical behavior. Among many fascinating [17,27,44–46] results that emerge from systems with one or more of these fields applied, it is predicted that h_4 is relevant whereas h_6 is not at some sufficiently high temperatures below the Kosterlitz-Thouless point [27]. The sixfold fields are expected to be present, for instance, in the otherwise Kosterlitz-Thouless-type two-dimensional melting of argon on a graphite substrate [47].

We performed a basic investigation of this result using our algorithm. Since we ran the algorithm at fairly high fields we did not choose reflections though the origin is uniform. Instead, we choose the planes of reflection first by rotating our starting spin by $\pi m/n$ for m uniformly taken from $1, \dots, n$ and generating a normal to the plane from that direction as described in Sec. IV B. The resulting susceptibilities as a function of system size are shown for various field strengths in Fig. 4. In the fourfold case, for each field strength there is a system size at which the divergence in the susceptibility is cut off, whereas for the sixfold case we measured no such cutoff

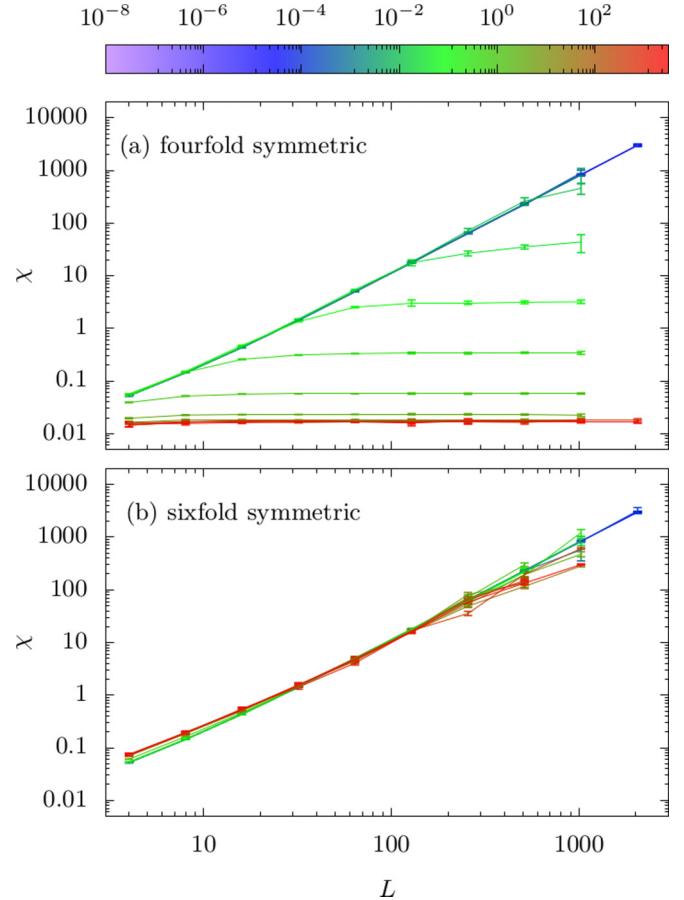


FIG. 4. Susceptibilities as a function of system size for a 2D $O(2)$ model at $T = 0.7$ and with (top) fourfold symmetric and (bottom) sixfold symmetric perturbing fields. The different field strengths are shown in different colors.

even up to strong fields. This conforms to the expected result that even in a strong field the sixfold perturbations preserve the critical behavior. Previous work has used Monte Carlo algorithms to investigate similar symmetry-breaking fields and used a hybrid cluster-metropolis method [17]. We applied a direct cluster method to this problem.

VII. CONCLUSIONS

We have taken several disparate extensions of cluster methods to spin models in an external field and generalized them to work for any model of a broad class. The resulting representation involves the introduction of not a ghost spin but a ghost transformation. We provide a C++ library with example implementations of all models described here [23]. We provided evidence that algorithmic extensions deriving from this method are the natural way to extend cluster methods in the presence of a field in the sense that they appear to reproduce the scaling of dynamic properties in a field that would be expected from renormalization group predictions.

In addition to uniting several extensions of cluster methods under a single description, our approach allows the application of fields not possible under prior methods. Instead of simply applying a spinlike field, this method allows for the application of *arbitrary functions* of the spins. For instance,

theoretical predictions for the effect of symmetry-breaking perturbations on spin models can be tested numerically [27,34,35,48].

ACKNOWLEDGMENTS

This work was supported by NSF Grant No. NSF DMR-1719490.

-
- [1] U. Wolff, *Nucl. Phys. B, Proc. Suppl.* **17**, 93 (1990).
 [2] W. Janke, *Math. Comput. Simul.* **47**, 329 (1998).
 [3] A. Coniglio and W. Klein, *J. Phys. A* **13**, 2775 (1980).
 [4] U. Wolff, *Phys. Lett. B* **228**, 379 (1989).
 [5] J. Du, B. Zheng, and J.-S. Wang, *J. Stat. Mech.: Theor. Exp.* (2006) P05004.
 [6] C.-W. Liu, A. Polkovnikov, and A. W. Sandvik, *Phys. Rev. B* **89**, 054307 (2014).
 [7] J.-S. Wang and R. H. Swendsen, *Physica A* **167**, 565 (1990).
 [8] U. Wolff, *Phys. Rev. Lett.* **62**, 361 (1989).
 [9] R. H. Swendsen and J.-S. Wang, *Phys. Rev. Lett.* **58**, 86 (1987).
 [10] C. F. Baillie and P. D. Coddington, *Phys. Rev. B* **43**, 10617 (1991).
 [11] A. Coniglio, F. d. Liberto, G. Monroy, and F. Peruggi, *J. Phys. A* **22**, L837 (1989).
 [12] Z. Alexandrowicz, *Physica A* **160**, 310 (1989).
 [13] J.-S. Wang, *Physica A* **161**, 249 (1989).
 [14] T. S. Ray and J.-S. Wang, *Physica A* **167**, 580 (1990).
 [15] C. Destri, F. Di Renzo, E. Onofri, P. Rossi, and G. P. Tecchiolli, *Phys. Lett. B* **278**, 311 (1992).
 [16] P. G. Lauwers and V. Rittenberg, *Phys. Lett. B* **233**, 197 (1989).
 [17] T. Ala-Nissila, E. Granato, K. Kankaala, J. M. Kosterlitz, and S.-C. Ying, *Phys. Rev. B* **50**, 12692 (1994).
 [18] O. Redner, J. Machta, and L. F. Chayes, *Phys. Rev. E* **58**, 2749 (1998).
 [19] L. Chayes, J. Machta, and O. Redner, *J. Stat. Phys.* **93**, 17 (1998).
 [20] J. Machta, M. E. J. Newman, and L. B. Chayes, *Phys. Rev. E* **62**, 8782 (2000).
 [21] V. Martin-Mayor and D. Yllanes, *Phys. Rev. E* **80**, 015701 (2009).
 [22] V. Martin-Mayor, B. Seoane, and D. Yllanes, *J. Stat. Phys.* **144**, 554 (2011).
 [23] J. Kent-Dobias, Wolff, <https://git.kent-dobias.com/wolff/>
 [24] S. Caracciolo, R. G. Edwards, A. Pelissetto, and A. D. Sokal, *Nucl. Phys. B* **403**, 475 (1993).
 [25] O. Loos, *Symmetric Spaces*, Mathematics lecture note series (Benjamin, New York, 1969).
 [26] H. Rieger, in *Annual Reviews of Computational Physics II Published*, edited by D. Stauffer (World Scientific, Singapore, 1995), pp. 295–341.
 [27] J. V. José, L. P. Kadanoff, S. Kirkpatrick, and D. R. Nelson, *Phys. Rev. B* **16**, 1217 (1977).
 [28] S. Caracciolo, R. G. Edwards, A. Pelissetto, and A. D. Sokal, *Nucl. Phys. B, Proc. Suppl.* **20**, 72 (1991).
 [29] U. Wolff, *Phys. Rev. Lett.* **60**, 1461 (1988).
 [30] C. M. Fortuin and P. W. Kasteleyn, *Physica* **57**, 536 (1972).
 [31] M. Hasenbusch, *Nucl. Phys. B* **333**, 581 (1990).
 [32] M. K. Bierbaum, <https://github.com/mattbierbaum/ising.js/>
 [33] I. Dimitrović, P. Hasenfratz, J. Nager, and F. Niedermayer, *Nucl. Phys. B* **350**, 893 (1991).
 [34] A. D. Bruce and A. Aharony, *Phys. Rev. B* **11**, 478 (1975).
 [35] D. Blankschtein and D. Mukamel, *Phys. Rev. B* **25**, 6939 (1982).
 [36] H. G. Evertz, M. Hasenbusch, M. Marcu, K. Pinn, and S. Solomon, *Phys. Lett. B* **254**, 185 (1991).
 [37] V. S. Dotsenko, W. Selke, and A. L. Talapov, *Physica A* **170**, 278 (1991).
 [38] G. Ossola and A. D. Sokal, *Nucl. Phys. B* **691**, 259 (2004).
 [39] A. B. Bortz, M. H. Kalos, and J. L. Lebowitz, *J. Comput. Phys.* **17**, 10 (1975).
 [40] F. Y. Wu, *Rev. Mod. Phys.* **54**, 235 (1982).
 [41] S. El-Showk, M. F. Paulos, D. Poland, S. Rychkov, D. Simmons-Duffin, and A. Vichi, *J. Stat. Phys.* **157**, 869 (2014).
 [42] R. Guida and J. Zinn-Justin, *J. Phys. A* **31**, 8103 (1998).
 [43] D. Stauffer, *Phys. Rep.* **54**, 1 (1979).
 [44] K. Kankaala, T. Ala-Nissila, and S.-C. Ying, *Phys. Rev. B* **47**, 2333 (1993).
 [45] S. B. Dierker, R. Pindak, and R. B. Meyer, *Phys. Rev. Lett.* **56**, 1819 (1986).
 [46] J. V. Selinger and D. R. Nelson, *Phys. Rev. Lett.* **61**, 416 (1988).
 [47] Q. M. Zhang and J. Z. Larese, *Phys. Rev. B* **43**, 938 (1991).
 [48] J. Manuel Carmona, A. Pelissetto, and E. Vicari, *Phys. Rev. B* **61**, 15136 (2000).